IEEE Access
Multidisciplinary | Rapid Review | Open Access Journal

Received May 15, 2020, accepted June 28, 2020, date of publication July 9, 2020, date of current version July 21, 2020.

Digital Object Identifier 10.1109/ACCESS.2020.3008252

Study of an SCSG-OSM for the Creation of an Urban Three-Dimensional Building

GUOQING ZHOU[1], (Senior Member, IEEE), TAO YUE[1], YU HUANG[2], BO SONG[1], KUNSHAN CHEN[1], (Fellow, IEEE), HONGCHANG HE[1], JINSHENG NI[3], LIQIANG ZHANG[4], (Member, IEEE), AND QIUYU PAN[1]

[1]Guangxi Key Laboratory for Spatial Information and Geomatics, Guilin University of Technology, Guilin 541004, China
[2]Nanning Exploration and Survey Geoinformation Institute, Nanning 530022, China
[3]Spatial Data Service Center, China Aerospace Science and Industry Corporation Ltd., Beijing 100048, China
[4]Faculty of Geographical Science, Beijing Normal University, Beijing 100875, China

Corresponding author: Guoqing Zhou (gzhou@glut.edu.cn)

This work was supported in part by the National Natural Science of China under Grant 41431179 and Grant 41961065, in part by the Guangxi Science and Technology Base and Talent Project under Grant Guike AD19254002, in part by the Guangxi Innovative Development Grand Grants under Grant GuikeAA18118038 and Grant GuikeAA18242048, in part by the Guangxi Natural Science Foundation for Innovation Research Team under Grant 2019GXNSFGA245001, in part by the National Key Research and Development Program of China under Grant 2016YFB0502501, in part by the Guilin Research and Development Plan Project under Grant 20190210-2, and in part by the BaGui Scholars Program of Guangxi.

ABSTRACT With the increasing needs of and rapid developments in digital and/or smart cities, an effective method for the management of various types of complex and massive buildings for the creation of a three-dimensional (3D) photorealistic city has become crucial for high-quality ''digital/smart city'' construction. To this end, this paper proposes a data model called the ''SCSG-OSM'', which combines spatial constructive solid geometry (SCSG) and the object-based spatial model (OSM). The SCSG-OSM assumes an object can be represented by four element types: point, line, face and body. The SCSG applies an extension of the dimensionally extended nine-intersection model (DE-9IM) to describe the spatial topological relationship. The OSM consists of nine definitions that define the points, lines, faces, and bodies of an object and applies point sets instead of node sets and face sets instead of surface sets to model buildings. Two data sets, depicting Denver, Colorado, USA, and Zurich, Switzerland, are employed to assess the storage space and the time consumption averages during the modelling of 3D buildings using the proposed data model. The experimental results demonstrate that the proposed SCSG-OSM is able to save storage space and reduce the computational time compared with the CSG-BR model, TIN model, POLYGON model, Patch model, SSM and CityGML model. Therefore, it can be concluded that the method proposed in this paper is a simple and effective method for the 3D photorealistic visualization of a large city.

INDEX TERMS Buildings, data models, digital photography, geospatial analysis, photorealism, urban areas, visualization.

I. INTRODUCTION

With the rapid developments and increasing needs of the construction of ''smart/digital cities'', high-quality three-dimensional (3D) models of buildings for photorealistic visualization are in great demand. This is typically an extremely cumbersome and time-consuming project for a large city with a large number of buildings. For this reason, many efforts seeking an effective method to represent 3D buildings have been proposed in recent years.

The associate editor coordinating the review of this manuscript and approving it for publication was Zhihan Lv.

II. RELATED WORK

A. 3D SPATIAL DATA MODELS FOR BUILDINGS

The representation of a building model typically uses a geometric representation method to describe the shape and structure of the building. A generating building model uses a suitable representation method and city data to generate a building that realistically conforms to the urban environment [1]. Four typical geometric representations used for

3D building models are the constructive solid geometry (CSG), boundary representation (B-Rep), surface representation and volume model [2]. For example, Zlatanova proposed a simple spatial model (SSM), which consists of 13 definitions that define the nodes, faces, points, lines, surfaces, and bodies of an object [3]. This method considers that an object can be represented through nodes and faces, eliminating the uniqueness of the relationship between arcs and faces in 3D space in which an arc segment is defined as part of more than two faces [4]. The SSM is effective for the spatial visualization and query of 3D buildings, but the conversion of points, lines, surfaces and bodies into nodes and faces in the SSM is time consuming. Vosselman and Suveg presented an automatic reconstruction method of 3D buildings based on the knowledge system of aerial imagery [5]. This method uses CSG to represent buildings. The complex buildings are regarded as a CSG tree, and its leaf nodes contain building models—voxels—whose internal nodes represent Boolean operations. Mao and Harrie proposed a method to summarize 3D buildings in 3D city models with different levels of detail and combined multiple levels of detail (LOD) for progressive distribution and visualization and multiple LODs for buildings. The extended structure BuildingTree supports single buildings and groups of buildings while creating representative CSG entities [6]. Zhou *et al.* proposed a hybrid modelling method for urban buildings based on texture data and spatial constructive solid geometry-boundary representation (SCSG-BR) [7]. This modelling method can effectively and rapidly create 3D buildings and spatial queries. With the proposed methods, building bodies are described by a surface or a boundary. These methods belong to the CSG model, which can represent complex buildings with little storage space. However, texture mapping becomes difficult because of the lack of definitions for boundaries and surfaces. Zhou *et al.* proposed an integrated method for representations of urban digital terrain models (DTM) and digital building models (DBM), with which a polygon is applied to represent the roof of a building and an object-oriented data structure is applied to represent a DBM [8]–[11]. Ledoux and Meijers focused on obtaining 'block-shaped' polyhedral representative buildings by squeezing building footprints [12]. Their algorithm can easily scale to very large data sets, but it lacks roof information. Sugihara generated 3D building models automatically by constructing rectified polygons on the basis of a geographic information system (GIS) and computer graphics (CG) [13] [14]. The methods mentioned above belong to the boundary representation model, which easily represents buildings with regular shapes but poorly represents buildings with irregular shapes. Xiong *et al.* analysed the topological properties of building surfaces and defined the basic elements of a building shape through loose nodes, loose edges and minimum periods. All buildings can be represented by combining these primitives, which simplifies the automatic modelling of building models [15]. Ohori *et al*. proposed a true 4D model method, for which a building can be seen as a single 4D object represented by a polyhedron [16]. Sun *et al.* applied volumetric analysis to create building models, with which voxelization is first created, and a layered distance map is generated [17]. This method belongs to the volume model, where the structure is simple and the topological relationship is clear. However, the storage space for the model is large, and the modelling processes are difficult.

B. 3D MODELLING METHODS AND TOOLS FOR BUILDINGS

Widely used methods and tools for the 3D modelling of buildings include ArcScene, AutoCAD, 3ds Max, SketchUp and the feature manipulation engine (FME). Kolbe *et al.*, Elmekawy *et al.*, Gröger and Plümer, Dore and Murphy, Goetz, and Slade *et al*. used city geography mark-up language (CityGML) to represent buildings [18]–[23]. Fan *et al.* combined semantic information and geometric information to model a building in which the generalization of 3D buildings with three LODs is first carried out using CityGML; then, the roof structure is adjusted to simplify the appearance of the surface, and finally, the typicalization of windows is established [24]. However, the problem encountered in practice is ''how many windows are suitable for visualization after typicalization''. Mao *et al*. proposed multiple representation data structures for the dynamic visualization of 3D city models called CityTree [25]. 3D city buildings are created by using different LODs [6], [26]–[36]. Löwner *et al*. proposed a different LOD concept for buildings [37]. Chen *et al*. proposed the so-called multisource recTification of gEometric Primitives (mSTEP) to improve building information model (BIM) reconstruction in high-density (HD) urban areas [38]. Xue *et al.* proposed a method based on optimization model generation (OMG) for the generation of a semantic BIM [39]. Wang and Li constructed 3D building models by extruding and stretching building data using 3D Max [40], [41]. Zhang mapped the outlines of buildings by using AutoCAD and established 3D building models by using 3ds Max [42]. Ma realized the vectorization of roofs for buildings by using ArcGIS, then added the height data of buildings and then established 3D building models by using ArcScene [43]. Zhang *et al*. proposed a triangular meshing algorithm based on additional constraint lines for hollow buildings and finally realized the modelling process in 3ds Max [44]. Although the methods and tools mentioned above have their own advantages, they also expose the following disadvantages: (1) a few methods are too simple; as a result, they occasionally fail to express the details of the buildings; (2) a few methods attempt to provide building details, but they are time consuming and require a large volume of data storage; and (3) many methods are easy to understand, but their data structures are relatively complicated and time consuming when implemented in practice.

For this reason, this paper proposes a method called the *SCSG-OSM*, which combines spatial constructive solid geometry (SCSG) and the object-based spatial model (OSM). The SCSG method improves the CSG model by using the dimensionally extended nine-intersection model (DE-9IM)

to represent the topological relations between buildings and determines the unique SCSG tree to represent the building. The DE-9IM is expanded to describe the topological relationship of two 3D bodies. Then, the OSM simplifies the SSM by using point elements instead of nodes or surfaces to represent lines, faces and bodies. Thus, the SCSG-OSM reduces the identifying procedures for nodes and surfaces, which can reduce both storage space and time consumption.

This paper is organized as follows. Section 3 provides a full description of the proposed SCSG-OSM. Section 4 presents the experiments and validations, and the conclusions are offered in Section 5.

III. PRINCIPLE OF THE SCSG-OSM

A. THE SCSG-OSM METHOD

Zlatanova and Gruber first defined the generalization of an *object* (*O*) and *composite object* (*CO*), in which each object was distinguished in accordance with its theme and geometry, and a further refinement was provided in the geometric domain [45]. This paper proposes a method called the *OSM*, which uses point sets instead of node sets and face sets instead of surface sets to model building data. The *OSM* proposed in this paper assumes that an object is represented by four element types: point, line, face and body. Therefore, a group of definitions must first be given below, which are different from the definitions given by Zlatanova [3].

1) PRINCIPLES OF A POINT

a: DEFINITIONS OF POINT (SUCH AS THE NODE OF A BUILDING)

A point is mathematically defined as $P_n = \{p\}, (n = 1, 2, 3\ldots)$, where P_n is an indexed set, and n is the unique index of a point. The characteristics are as follows:

a) The interior of a point, represented by P_n°, is an empty set, *i.e.*, $P_n^\circ = \emptyset$. The boundary of a point, noted by ∂P_n, is itself. The closure of a point, represented by $\overline{P_n}$, is a union between P_n° and ∂P_n, mathematically expressed by $\overline{P_n} = P_n \cup \partial P_n$.

b) The exterior of a point, represented by $P_n^- = U - \overline{P_n}$, is the difference between the universe U and $\overline{P_n}$ and mathematically expressed by $P_n^- = U - \overline{P_n}$.

b: RULES OF POINTS IN TOPOLOGICAL SPACE FOR THE SCSG-OSM

According to the definitions above, we make rules of points in topological space for the SCSG-OSM. If the topological space of points is represented by $\wedge$, which consists of *ppn* points and whose family set is noted by *PD*, then they can mathematically be expressed by

$$PD = \{P_n\} = \bigcup_{n=1}^{ppn} P_n, \{P_n\} \subset \wedge, \quad 1 \le n \le ppn \tag{1}$$

The characteristics are as follows:

If the intersection of *ppn* points is an empty set and mathematically expressed by

$$\left(\bigcup_{m=1}^{ppn} P_m\right) \cap \left(\bigcup_{n=m+1}^{ppn} P_n\right) = \emptyset \tag{2}$$

then there exist two points, P_m and P_n, which are disjoint and are the subsets of *PD*.

a) If the intersection of *ppn* points is not an empty set and mathematically expressed by

$$\left(\bigcup_{m=1}^{ppn} P_m\right) \cup \left(\bigcup_{n=m+1}^{ppn} P_n\right) = \emptyset \tag{3}$$

then there exist two identical points.

b) If the intersection of the two points P_m and P_n is an empty set, then the two points are disjoint. This can be mathematically expressed by

$$P_m \cap P_n = \emptyset \tag{4}$$

2) PRINCIPLES OF A LINE

a: DEFINITIONS OF LINE (SUCH AS THE OUTLINE OF A BUILDING)

A line is mathematically defined as

$$L_i = \{P_n^{l_p}\} = \bigcup_{l_p=1}^{k} P_n^{l_p}, \quad (i = 1, 2, 3, \ldots) \tag{5}$$

where L_i is an indexed set containing k points $P_n, 2 \le k \le ppn$, l_p is the unique line index of a point, and *ppn* is the total number of points. The characteristics are as follows:

a) If there exists a line, then there must exist a corresponding pair of points, denoted by $P^{ft_p} \in L_i$ and $P^{lt_p} \in L_i$, which represent the first point and the last point, respectively. If the pair of points is not equal, the line is disconnected; otherwise, the line is enclosed.

b) A line, noted by $L_i (i = 1, 2, 3, \ldots)$, consists of many connected pairs of points in order, and the connected pair of points are not the same point, *i.e.*, $(P^{l_p}, P^{x_p}) \neq (P^{ft_p}, P^{lt_p})$. This can be mathematically expressed by

$$(P^{l_p}, P^{x_p}) \in L_i \tag{6}$$

c) A line, denoted by $(P^r, P^s, P^t) \in F_i$, consists of many connected pairs of points in order; the intersection of each pair of points is empty. This can be mathematically expressed by

$$\cup_{l_p}^{k} = \left({}_1P^{l_p}\right) \cap \left(\cup_{x_p}^{k} = l_p + 1P^{x_p}\right) = \phi \tag{7}$$

where $P^{l_p} \in L_i, P^{x_p} \in L_i$ represent each pair of points.

d) The interior of a line, represented by L_i°, is the difference between the closure of k points and the union of the first point $\overline{P^{ft_p}}$ and the last point $\overline{P^{lt_p}}$. This can be mathematically expressed by

$$L_i^\circ = \left(\bigcup_{l_p=1}^{k} \overline{P_n^{l_p}}\right) - \left(\overline{P^{ft_p}} \cap \overline{P^{lt_p}}\right) \tag{8}$$

e) The boundary of a line, denoted by ∂L_i, is the difference between the closure of a line $\overline{L_i}$ and the interior of a line L_i°, or is the union set between the closure set of the first point $\overline{P^{ft_p}}$ and the last point, $\overline{P^{lt_p}}$. This can be mathematically expressed by

$$\partial L_i = \overline{L_i} - L_i^\circ \text{ or } \partial L_i = \overline{P^{ft_p}} \cup \overline{P^{lt_p}} \tag{9}$$

f) The closure of a line, denoted by $\overline{L_i}$, is the union set of the closure of k points. This can be mathematically expressed by

$$\overline{L_i} = \bigcup_{l_p=1}^{k} \overline{P_n^{l_p}}, \quad \{P_n^{l_p}\} = L_i \tag{10}$$

g) The exterior of a line, represented by $A^- \cap B^-$, is the difference between the universe U and the closure of a line $\overline{L_i}$. This can mathematically be expressed by $L_i^- = U - \overline{L_i}$.

b: RULES OF LINES IN TOPOLOGICAL SPACE FOR THE SCSG-OSM

According to the definitions above, we make rules of lines in topological space for the SCSG-OSM. If the topological space of lines, denoted by $\wedge$, has *lpn* lines and a family set, denoted by *LP*, then they can be mathematically expressed by

$$LP = \{L_i\} = \bigcup_{i=1}^{lpn} L_i, \{L_i\} \subset \wedge, \quad 1 \le i \le lpn \tag{11}$$

where i is the unique index of a line. P_n is the point of L_i, and n is the unique index of a point. The characteristics are as follows:

a) If the intersection of *lpn* lines is not an empty set, then at least one point of one of the lines is equal to the point in the other line. This can be mathematically expressed by

$$\left(\bigcup_{g=1}^{lpn} L_g\right) \cap \left(\bigcup_{h=g+1}^{lpn} L_h\right) \neq \emptyset \tag{12}$$

Then, $P_1 = P_2$, $P_1 \in L_g$, and $P_2 \in L_h$.

b) If the intersection between points P_n with other points in a line, denoted by $\{P^{l_p}\} = L_i$, is empty, then the point P_n and the line L_i are disjoint. This can be mathematically expressed by

$$P_n \cap \left(\bigcup_{l_p=1}^{k} P^{l_p}\right) = \emptyset, \quad 2 \le k \le lpn \tag{13}$$

Otherwise, the two points belong to part of the same line.

3) PRINCIPLES OF FACE

a: DEFINITIONS OF FACE (SUCH AS THE ROOF OF A BUILDING)

A face is mathematically defined as

$$F_i = \{P_n^{f_p}\} = \bigcup_{f_p=1}^{k} P_n^{f_p}, \quad (i = 1, 2, 3 \ldots, n) \tag{14}$$

where F_i is an indexed set (such as the walls of a building) containing k ordered points, where $3 \le k \le ppn$, *ppn* is the total number of points, and f_p is the unique face index of a point specifying the current order in a face. P_n are the points of F_i, and n is the unique index of a point. The characteristics are as follows:

a) F_i is a connected set that contains ordered pair points

$$(P^{f_p}, P^{f_p+1}) \in F_i, \quad 1 \le f_p \le k \tag{15}$$

b) If the intersection of points in the face is an empty set, then there are not two equal points in a face. This can be mathematically expressed by

$$\left(\bigcup_{f_p=1}^{k} P^{f_p}\right) \cap \left(\bigcup_{f_x=f_p+1}^{k} P^{f_x}\right) = \emptyset \tag{16}$$

where $\{P^{f_p}\} = F_i$.

c) If a face is planned, for each triple of points, $P^r, P^s, P^t (P^r \in F_i, P^s \in F_i, P^t \in F_i)$ where r, s, and t are the order of the point sets and $r \neq s \neq t$, then a unique equation $ax + by + cz + d = 0$ is satisfied in IR^3, where a, b, c, and d are constants, and (x, y, z) is the position of the points.

d) At least one (or more) triple of the ordered points $(P^r, P^s, P^t) \in F_i$, where r, s, and t are the order of the point sets, does not satisfy the equation $ax+by+cz = g$ in IR^3, where a, b, c, and g are constants, and (x, y, z) is the position of the points.

e) In IR^3, all k points, denoted by $\{P^{f_p}\} = F_i$, $1 < f_p < k$, are counter-clockwise. For example, each of the ordered triple points $(P^r, P^s, P^t) \in F_i$, where r, s, and t are the order of the point sets and $r < s < t$, satisfies a planar equation, $ax+by+cz+d = 0$, where a, b, c, and d are constant, and (x, y, z) is the position of the points, with which there exists a normal vector $n = (a, b, c)$.

f) If three points are denoted by $p_i \in P^r, p_j \in P^s, p_k \in P^t$ in IR^3, where $(P^r, P^s, P^t) \in F_i$ are ordered triple points, r, s, and t are the order of the point sets, and i, j, and k are the order of the points, the angle $\alpha = (u, v)$, where $u = \overrightarrow{p_i, p_j}, v = \overrightarrow{p_i, p_k}, (0 < \alpha \le 2\pi)$, and then F_i is convex.

g) The interior of a face, represented by F_i°, is an enclosed area by the point sets. The boundary of a face, represented by ∂F_i, is the union of all connected points and is expressed by $P_n \in F_i$. The point set $\{P_{f_p}\} = F_i$ is a subset of the boundary of a face. This can be

mathematically expressed by

$$\{P_1, \ldots, P_{f_p}\} \subset \partial F_i, \quad \partial F_i = \cup_{f_p=1}^{k} P^{f_p} \tag{17}$$

h) The closure of a face, represented by $\overline{F_i}$, is the union set between ∂F_i and F_i°. This can mathematically be expressed by $\overline{F_i} = \partial F_i \cup F_i^\circ$.

i) The exterior of a face, represented by F_i^-, is the difference between the universe U and the closure of a face $\overline{F_i}$. This can be mathematically expressed by

$$F_i^- = U - \overline{F_i} \tag{18}$$

b: RULES OF FACES IN TOPOLOGICAL SPACE FOR THE SCSG-OSM

According to the definitions above, we make rules of faces in topological space for the SCSG-OSM. If the topological space of faces is denoted by $\wedge$, which consists of *fpn* faces and whose family set is noted by *FL*, then they can be expressed by

$$FL = \{F_i\} = \bigcup_{i=1}^{fpn} F_i, \{F_i\} \subset \wedge, \quad 1 \le i \le fpn \tag{19}$$

where i is the unique index of a face, P_n is the points of F_i, and n is the unique index of a point. The characteristics are as follows:

a) If the intersection of all *fpn* faces is an empty set, then there are no two equal faces. This is mathematically expressed by

$$\left(\bigcup_{g=1}^{fpn} F_g\right) \cap \left(\bigcup_{h=g+1}^{fpn} F_h\right) = \emptyset \tag{20}$$

b) If the intersection of a point $P_y \in PD$ with another point in the face $P^{f_p} \in F_x$ is an empty set, then a point $P_y \in PD$ and a face $F_x \in FL$ are disjoint; otherwise, point P_y is a part of the face F_x. This can be mathematically expressed by

$$\left(\bigcup_{f_p=1}^{k} P_y\right) \cap P^{f_p} = \emptyset \tag{21}$$

c) If the intersection of each pair of points, denoted by $P^{f_p 1} \in F_{x1}$ and $P^{f_p 2} \in F_{x2}$, is an empty set, then the two faces F_{x1} and F_{x2} are disjoint. This is mathematically expressed by

$$\left(\bigcup_{f_p 1=1}^{y1} P^{f_p 1}\right) \cap \left(\bigcup_{f_p 2=1}^{y2} P^{f_p 2}\right) = \emptyset \tag{22}$$

d) If the intersection of all *fpn* faces is set of the points, expressed by

$$\left(\bigcup_{g=x1}^{x} F_g\right) \cap \left(\bigcup_{h=x3}^{x} F_h\right) = (P^{f_p 1}, \ldots, P^{f_p 2}) \tag{23}$$

where $2 \le x \le fpn - 2$, $x3 = x2 - x1 + 1$, and $(P^{f_p 1}, \ldots, P^{f_p 2})$ is each tuple of ordered points, and $(F_{x1}, \ldots, F_{x2}) \in FL$ are the faces in FL, then the faces $F_{x1}, \ldots, F_{x2}$ strongly meet at points $P_{y1}, \ldots, P_{y2}$, where $2 \le (y2 - y1) \le ppn - 2$. If $y2 - y1 = 0$, *i.e.*, the intersection has only a unique element P_y, then the faces $F_{x1}, \ldots, F_{x2}$ weakly meet at the point $4 \le k \le fpn$. If $y2 - y1 = 1$, *i.e.*, the intersection has only two points, then they are considered as a pair of the ordered points in each face of the intersection.

e) If the intersection of each pair of points P^{l_p}, P^{x_p} is an empty set, expressed by

$$\{P^{l_p}\} \subset L_i, \{P^{x_p}\} \subset F_i \tag{24}$$

Then, $\{L_i\}$ and $\{F_i\}$ are disjoint. This is mathematically expressed by

$$\left(\bigcup_{l_p=1}^{k1} P^{l_p}\right) \cap \left(\bigcup_{x_p=1}^{k2} P^{x_p}\right) = \emptyset, \quad 2 \le k1 \le lpn, \quad 3 \le k2 \le fpn \tag{25}$$

f) For some lines $L_i \subset LP$, if there exists a set of points, *i.e.*, $\{P_n, \ldots, P_y\} \subset PD$ and $\{P_n^{l_p}, \ldots, P_y^{l_p}\} \subset L_i$, which satisfy the conditions $\{P_n^{f_p}, \ldots, P_y^{f_p}\} \subset F_i$ and $\{F_i\} \subset FL$, then the line L_i strongly meets the face F_i. If the intersection of the points contains a unique element P_x, then the line L_i weakly meets the face F_i at P_x.

g) If the points, denoted by $\{P_n, \ldots, P_y\} \subset L_i$, are the boundary of a face, *i.e.*, $\{P_n, \ldots, P_y\} \subset F_i$, then the interior of the face F_j does not contain the set of lines L_i.

4) PRINCIPLES OF BODY

a: DEFINITIONS OF BODY (SUCH AS A BUILDING)

A body is mathematically defined as

$$B_b = \{F_i^{b_f}\} = \bigcup_{b_f=1}^{k} F_i^{b_f}, \quad (b = 1, 2, 3, \ldots) \tag{26}$$

where B_b is an indexed set (such as several buildings) containing k faces of F_i, $4 \le k \le fpn$, $1 \le i \le k$, *fpn* is the total number of faces, b_f is the unique body index of a face, and F_i is the faces of B_b. The characteristics are as follows:

a) The points of a body can be expressed by

$$B_b = \bigcup_{b_f=1}^{k1} F_i^{b_f} = \bigcup_{b_f=1}^{k1} \bigcup_{f_p=1}^{k2} P_n^{b_f, f_p} \tag{27}$$

where each point $P^n \in B_b$ belongs to at least three faces $F_x \in B_b$, $F_y \in B_b$, and $F_z \in B_b$, *i.e.*, $P^n \in F_x$, $P^n \in F_y$, and $P^n \in F_z$. For an ordered pair of points $(P^n, P^{n+1}) \in B_b$ and two faces $F_x \in B_b$, $F_y \in B_b$, we have

$$(P^n, P^{n+1}) \in F_x, (P^{n+1}, P^n) \in F_y \tag{28}$$

b) The interior of a body, denoted by B_b°, is an enclosed space constructed by k faces $\{F_i^{b_f}\} = B_b$. The boundary of a body, represented by ∂B_b, is the closure of all the

faces, denoted by $\{F_i^{b_f}\} = B_b$. This is mathematically expressed by

$$\partial B_b = \bigcup_{b_f=1}^{k} \overline{F_i^{b_f}} \tag{29}$$

The closure of a body, represented by $\overline{B_b}$, is a union between B_b° and ∂B_b and is expressed by $\overline{B_b} = B_b^\circ \cup \partial B_b$.

c) The exterior of a body, represented by B_b^-, is the difference between the universe U and the closure of a body $\overline{B_b}$. This is mathematically expressed by

$$B_b^- = U - \overline{B_b} \tag{30}$$

b: RULES OF BODIES IN TOPOLOGICAL SPACE FOR THE SCSG-OSM

According to the definitions above, we make rules of bodies in topological space for the SCSG-OSM. If the topological space of a body is denoted by $\wedge$, which has *bfn* bodies and whose family set is denoted by BF, then they can be mathematically expressed by

$$BF = \{B_b\} = \bigcup_{b=1}^{bfn} B_b, \{B_b\} \subset \wedge, \quad 1 \le b \le bfn \tag{31}$$

where b is the unique index of a body. F_i represents the faces of B_b, where i is the unique index of a face. The characteristics are as follows:

a) If the intersection of *bfn* bodies is not an empty set, expressed by

$$\left(\bigcup_{g=1}^{bfn} B_g\right) \cap \left(\bigcup_{h=g+1}^{bfn} B_h\right) \neq \emptyset \tag{32}$$

then equal faces may exist from different bodies. That is, for some faces F_i and pairs of bodies B_g, B_h, there are

$$\{F_i\} \subset B_g, \{F_i\} \subset B_h \tag{33}$$

b) If the intersection of each face $\{F^{b_f}\} = B_b$ is an empty set, expressed by

$$\left(\bigcup_{b_f=1}^{k} F_i\right) \cap \left(F^{b_f}\right) = \emptyset, \quad 3 \le k \le bfn \tag{34}$$

then body $\{B_b\} \subset BF$, and face $\{F_i\}$ is disjoint. Otherwise, the face is the part of the body.

c) If there is a body B_j with many faces F_i that satisfies $\{F_i\} \subset B_j^\circ$, then the faces are *inside* of the body.

d) If there is a body B_j with many points P_n that satisfies $\{P_n\} \subset B_j^\circ$, then the points are *inside* of the body.

5) THE RELATIONSHIPS OF ALL THE ELEMENTS

a: THE RELATIONSHIPS OF THE ELEMENTS

If the topological space of all the elements is denoted by $\wedge$, which has *xf* faces inside a body and *xp* points inside the same body, the family set of the *xf* faces is denoted by XF and the family set of the *xp* points is denoted by XP, then they can be mathematically expressed by:

$$XF = \{F_i^{fib}\} = \bigcup_{fib=1}^{xf} F_i^{fib} \tag{35}$$

where *fib* is the face-in-body index of the point, and

$$XP = \{P_n^{nib}\} = \bigcup_{nib=1}^{xp} P_n^{nib} \tag{36}$$

where *nib* is the point-in-body index of the point.

B. THE 3D TOPOLOGICAL RELATIONSHIP IN THE SCSG-OSM

The nine-intersection model (9IM) was originally presented by Erné [46]. This is applied to describe the topological relationship of the elements described above. The 9IM describes topological relationships using the nine intersections formed by the boundaries, interiors and exteriors of two spatial objects. Suppose that there are two spatial objects, A and B, which use $\partial A/A^\circ/A^-$ and $\partial B/B^\circ/B^-$ to represent their boundaries, interiors and exteriors, respectively. The intersections of $\partial A/A^\circ/A^-$, $\partial A/A^\circ/A^-$ and $\partial B/B^\circ/B^-$ form a 9IM matrix. The tuples in the matrix of the 9IM have many null ($\emptyset$) and nonempty ($\neg\emptyset$) values. Null ($\emptyset$) means separation, and nonempty ($\neg\emptyset$) means intersection. Theoretically, there are $2^9 = 512$ possible values for the intersections of the interior, the exterior and the boundaries in total, but some of the values do not exist in reality, so only some of the topological relationships remain after filtering out the conditions.

With the given definitions and rules above, this paper gives 11 important topological relationships among bodies (also see Fig. 1). The detailed descriptions are given below.

R031 represents the topological relationship in which A and B are disjoint (see Fig. 1 (a)). This is the most easily identifiable relationship using their boundaries. If the intersection of the boundaries of A and B is an empty set, then A and B are disjoint. This means that if $\{\{F_1\} \ldots \{F_i\}\} = \partial A, \{\{F_1\} \ldots \{F_j\}\} = \partial B$, then

$$\left(\bigcup_{g=1}^{i} F_g\right) \cap \left(\bigcup_{h=1}^{j} F_h\right) = \emptyset \tag{37}$$

R179 represents the topological relationship that A is inside B (see Fig. 1 (b)). If the boundary of A is the subset of the interior of B, *i.e.*, $\partial A \subset B^\circ$, then A is inside B. This means that if $\{\{F_1\} \ldots \{F_i\}\} = \partial A, \{\{F_1\} \ldots \{F_j\}\} = B^\circ$, then

$$\left(\bigcup_{g=1}^{i} F_g\right) \cap \left(\bigcup_{h=1}^{j} F_h\right) = \bigcup_{g=1}^{i} F_g \tag{38}$$

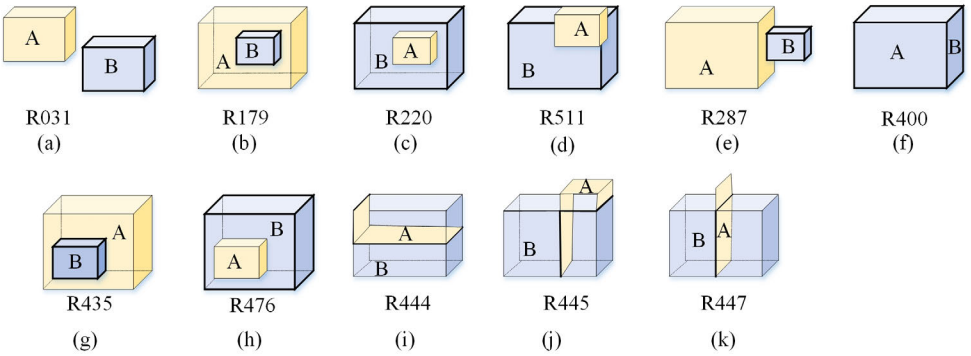

FIGURE 1. Eleven topological relationships of bodies.

R220 represents the topological relationship that B contains A (see Fig. 1 (c)). This has the same representation as R179.

R511 represents the topological relationship in which A overlaps B (see Fig. 1 (d)). This relationship is for an analysis of the equal faces. If the boundary of A is equal to the interior of B, then A overlaps B. This means that if $\{\{F_1\}\ldots\{F_i\}\} = \partial A$, $\{\{F_1\}\ldots\{F_j\}\} = B^\circ$, then

$$\bigcup_{g=1}^{i} F_g = \bigcup_{h=1}^{j} F_h \Rightarrow \mathrm{g} = h \tag{39}$$

R287 represents the topological relationship that A meets B (see Fig. 1 (e)). The intersection of two bodies can be faces, lines and points.

R400 represents the topological relationship that A equals B (see Fig. 1 (f)). If the boundary of A is equal to the boundary of B, then A is equal to B. This means that if $\{\{F_1\}\ldots\{F_i\}\} = \partial A$, $\{\{F_1\}\ldots\{F_j\}\} = \partial B$, then

$$A^\circ \cap \partial B \Rightarrow \mathrm{g} = h \tag{40}$$

R435 represents the topological relationship that A covers B (see Fig. 1 (g)). The covered body must contain three or more faces and is expressed by $\partial B \subset A^\circ$.

R476 represents the topological relationship that A is covered by B (see Fig. 1 (h)). This satisfies the relationship $\partial A \subset B^\circ$.

R444, **R445** and **R447** represent the topological relationship in which face A is covered by body B (see Fig. 1 (i), (j) and (k)).

To realize this spatial topological relationship using a computer, a binary code is applied to represent the topological relationship, in which "1" represents the intersection of two objects, and "0" represents the non-intersection of two objects. For example, if there are two-point objects that are noted A and B, respectively, the intersect between the boundaries of A and B is expressed as ∂A and ∂B, the internal of A and B is expressed as A° and B°, and the external of A and B is expressed as A^- and B^-; their binary codes are determined using the 9I model matrix method, *i.e.*, when the boundary of A does not intersect with the boundary of B, $\partial A \cap \partial B$ is equal to "0". Similarly, $A^\circ \cap B^\circ$ may be equal to "0", $\partial A \cap B^\circ$ may be equal to "0", $A^\circ \cap \partial B$ may be equal to "0", $A^- \cap B^-$ may be equal to "1", $A^- \cap \partial B$ may be equal to "1", $A^- \cap B^\circ$ may be equal to "0", $\partial A \cap B^-$ may be equal to "1", and $A^\circ \cap B^-$ may be equal to "0". With the rule formulated above, the binary code of the possible topological relationship for A and B is "000011010", and its decimal value is 026. Thus, *R026* represents the topological relationship, as also shown in Fig. 2(a1). The possible topological relationships, as shown in Figs. 1, 2 and 3, are listed in Table 1.

As observed from Figs. 1, 2, and 3, eight types of major topological relationships exist. They are disjoint, met, contained, inside, covered, covered by, overlapped, and equal.

C. THE ORGANIZATION OF DATA SETS IN THE SCSG-OSM

The organization of data for implementation of the SCSG-OSM can be illustrated using Fig. 4. The points are represented by coordinates X, Y, and Z, and a point set (and/or point sets) is applied to represent a line (or lines), a face (or faces) and a body (or bodies), which construct a geometric object (GO). The GO can be described using a geometric description (Dsc) and its attributes (Atts). Each point, line, face and body is assigned a unique ID, denoted by "*PID*", "*LID*", "*FID*" and "*BID*", respectively. The topographic relationship, denoted by "R", of the possible object exists in two types: faces in a body and points in a body, all of which are also presented by the point sets.

To further explain the organization of data in the SCSG-OSM, a complicated building is taken as an example and shown in Fig. 5(a). The building consists of 24 points, which are grouped as the root of three-point sets, denoted by P_1, P_2 and P_3, *i.e.*, P_1 consists of p_1-p_8, P_2 consists of p_9-p_{16} and P_3 consists of p_{17}-p_{24}. Their expressions are

$$PD = \{P_1, P_2, P_3\} = \{\{p_1, \ldots., p_8\}, \{p_9, \ldots., p_{16}\}, \{p_{17}, \ldots., p_{24}\}\} \tag{41}$$

where PD presents the point sets in the topological space described in "Section III.A.1".

The point sets further construct line sets (see Fig. 5(a)), denoted by L_1, L_2 and L_3, in which L_1 consists of l_1-l_{12},

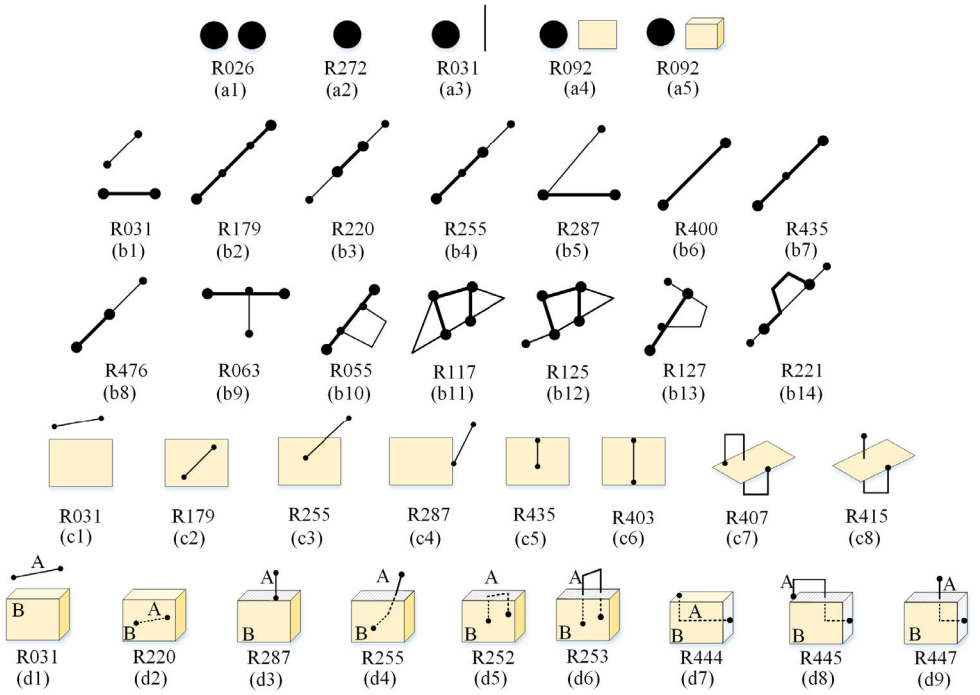

FIGURE 2. Thirty-six important topological relationships of points and lines.

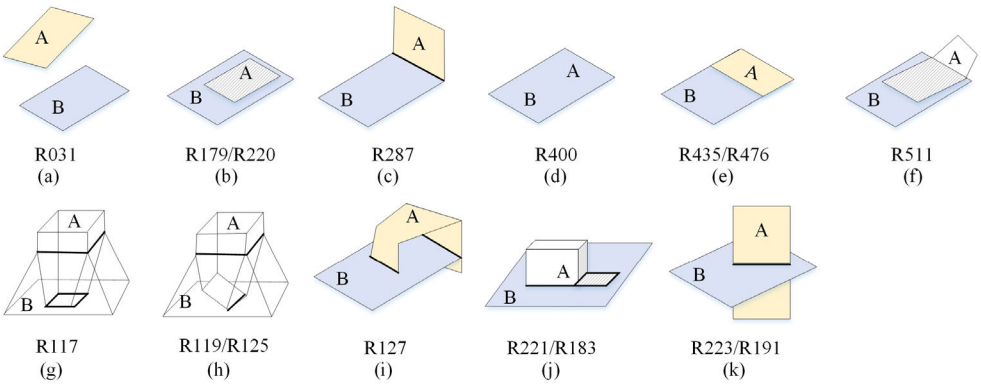

FIGURE 3. Eleven important topological relationships of faces and faces.

L_2 consists of l_{13}-l_{24} and L_3 consists of l_{25}-l_{36} and is mathematically expressed by

$$LP=\{L_1, L_2, L_3\}=\{\{l_1, \ldots., l_{12}\}, \{l_{13}, \ldots., l_{24}\}, \{l_{25}, \ldots., l_{36}\}\}=\{P_1, P_2, P_3\}=\{\{p_1, \ldots., p_8\}, \{p_9, \ldots., p_{16}\}, \{p_{17}, \ldots., p_{24}\}\} \quad (42)$$

where LP presents the line sets in the topological space described in "Section III.A.2".

The line sets further construct face sets (see Fig. 5(b)), denoted by F_1, F_2 and F_3, in which F_1 consists of f_1-f_6, F_2 consists of f_7-f_{11} and F_3 consists of f_{12}-f_{16} and is mathematically expressed by

$$\begin{aligned} FL=\{F_1,F_2,F_3\}&=\{\{f_1,\ldots,f_6\},\{f_7,\ldots,f_{11}\},\{f_{12},\ldots,f_{16}\}\} \\ &=\{L_1,L_2,L_3\}=\{\{l_1,\ldots.,l_{12}\},\{l_{13},\ldots.,l_{24}\},\{l_{25},\ldots.,l_{36}\}\} \\ &=\{P_1,P_2,P_3\}=\{\{p_1,\ldots.,p_8\},\{p_9,\ldots.,p_{16}\},\{p_{17},\ldots.,p_{24}\}\} \end{aligned} \quad (43)$$

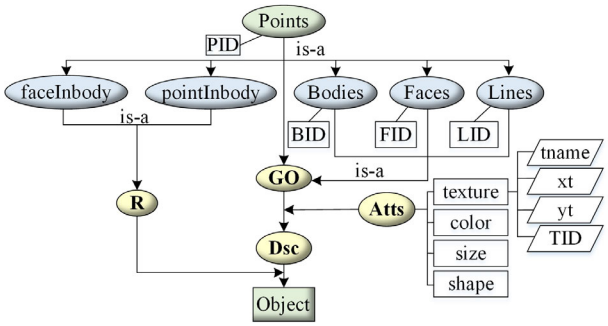

FIGURE 4. The organization of data in the SCSG-OSM.

where FL presents the face sets in the topological space described in "Section III.A.3".

Furthermore, the face sets construct bodies, denoted by b_1, b_2 and b_3, which construct a building (see Fig. 5(c)).

TABLE 1. Topological relationships (B represents body, F represents face, L represents line, P represents point, "-" indicates non-existent topological relationship, and "Y" indicates a possible topological relationship).

Binary	Decimal	B/B	B/F	B/L	B/P	F/F	F/L	F/P	L/L	L/P	P/P	Topological relationship	Figures
000011010	R026	-	-	-	-	-	-	-	-	-	Y	disjoint	Fig. 2 (a1)
000011111	R031	Y	Y	Y	-	Y	Y	-	Y	Y	-	disjoint	Fig. 1 (a)/Fig. 2(a3) (b1)(c1) (d1)/Fig. 3 (a)
000110111	R055	-	-	-	-	-	-	-	Y	-	-	met	Fig. 2 (b10)
000111111	R063	-	-	-	-	-	-	-	Y	-	-	met	Fig. 2 (b9)
001011101	R092	-	-	-	Y	-	-	Y	-	-	-	disjoint	Fig. 2 (a4)(a5)
001110101	R117	-	-	-	-	Y	-	-	Y	-	-	met	Fig. 2 (b11)/Fig. 3 (g)
001110111	R119	-	-	-	-	Y	-	-	-	-	-	met	Fig. 3 (h)
001111101	R125	-	-	-	-	Y	-	-	Y	-	-	met	Fig. 2(b12)/Fig. 3 (h)
001111111	R127	-	-	-	-	Y	-	-	Y	-	-	met	Fig. 2(b13)/Fig. 3(i)
010110011	R179	Y	-	-	-	Y	Y	-	Y	-	-	contained	Fig. 1(b)/Fig. 2(b2) (c2)/Fig. 3(b)
010110111	R183	-	-	-	-	Y	-	-	-	-	-	inside	Fig. 3(j)
010111111	R191	-	-	-	-	Y	-	-	-	-	-	inside	Fig. 3(k)
011011100	R220	Y	-	Y	-	Y	Y	-	Y	-	-	inside	Fig. 1(c)/Fig. 2(b3) (d2)/Fig. 3(b)
011011101	R221			-	-	Y			Y			contained	Fig. 2(b14)/Fig. 3(j)
011011111	R223	-	-	-	-	Y	-	-	-	-	-	contained	Fig. 3(k)
011111100	R252	-	-	Y	-	-	-	-	-	-	-	overlapped	Fig. 2(d5)
011111101	R253	-	-	Y	-	-	-	-	-	-	-	overlapped	Fig. 2(d6)
011111111	R255	-	-	Y	-	-	Y	-	Y	-	-	overlapped	Fig. 2(b4) (c3) (d4)
100010000	R272	-	-	-	-	-	-	-	-	-	Y	met	Fig. 2(a2)
100011111	R287	Y	-	Y	-	Y	Y	-	Y	-	-	met	Fig. 1(e)/Fig. 2(b5) (c4) (d3)/Fig. 3(c)
110010000	R400	Y	-	-	-	Y	-	-	Y	-	-	equal	Fig. 1(f)/Fig. 2(b6)/Fig. 3(d)
110010011	R403	-	-	-	-	-	Y	-	-	-	-	inside	Fig. 2(c6)
110010111	R407	-	-	-	-	-	Y	-	-	-	-	inside	Fig. 2(c7)
110011111	R415	-	-	-	-	-	Y	-	-	-	-	equal	Fig. 2(c8)
110110011	R435	Y	-	-	-	Y	Y	-	Y	-	-	covered	Fig. 1(g)/Fig. 2(b7) (c5)/Fig. 3(e)
110111100	R444	-	Y	Y	-	-	-	-	-	-	-	covered	Fig. 1(i)/Fig. 2(d7)
110111101	R445	-	Y	Y	-	-	-	-	-	-	-	covered	Fig. 1(j)/Fig. 2(d8)
110111111	R447	-	Y	Y	-	-	-	-	-	-	-	covered	Fig. 1(k)/Fig. 2(d9)
111011100	R476	Y	-	-	-	Y	-	-	Y	-	-	covered by	Fig. 1(h)/Fig. 2(b8)/Fig. 3(e)
111111111	R511	Y	-	-	-	Y	-	-	-	-	-	overlapped	Fig. 1(d)/Fig. 2(f)

Mathematically, this can be expressed by

$$BF=\{b_1,b_2,b_3\}=\{F_1,F_2,F_3\}=\{\{f_1,\ldots,f_6\},\{f_7,\ldots,f_{11}\},\{f_{12},\ldots,f_{16}\}\}=\{L_1,L_2,L_3\}=\{\{l_1,\ldots,l_{12}\},\{l_{13},\ldots,l_{24}\},\{l_{25},\ldots,l_{36}\}\}=\{P_1,P_2,P_3\}=\{\{p_1,\ldots,p_8\},\{p_9,\ldots,p_{16}\},\{p_{17},\ldots,p_{24}\}\} \quad (44)$$

where BF presents the body sets in the topological space described in "Section III.A.4".

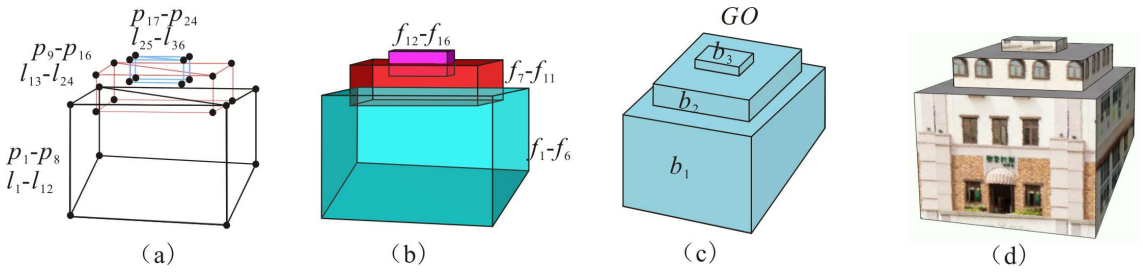

FIGURE 5. Example of the organization of data for a building in the SCSG-OSM.

With the above descriptions in this section, the GO is constructed and is depicted in Fig. 5(c). The Atts, which include their texture, colour, size and shape, are attached in Fig. 5(c) and depicted in Fig. 5(d). The two types of relationships, faces in a body and points in a body, are also illustrated in Fig. 5(a), Fig. 5(b), and Fig. 5(c), *i.e.*, faces f_1-f_6 are in body b_1, faces f_7-f_{11} are in body b_2, and faces f_{12}-f_{16} are in body b_3. Additionally, points p_1-p_8 are in body b_1, points p_9-p_{16} are in body b_2, and points p_{17}-p_{24} are in body b_3. With the organization of the data presented here, a photorealistic building is finally constructed with its geometric descriptions, attributes and topographic relationships (see Fig. 5(d)).

D. DISCUSSION AND COMPARISON ANALYSIS BETWEEN SSM AND SCSG-OSM

To further help understand the differences between the SSM proposed by Zlatanova and the SCSG-OSM proposed in this paper, this section provides a further discussion and comparisons [3]. The major contributions of the SSM proposed by Zlatanova are as follows:

a) The SSM consists of 13 definitions that define the nodes, faces, points, lines, surfaces, and bodies of an object. This means that the SSM considers that an object is represented through nodes and faces.
b) The SSM eliminates the relationship between arcs and faces, *i.e.*, an arc segment can be part of more than two faces.
c) The SSM explicitly stores the relationships of node-in-face and face-in-body, the direction of the faces, and the order of the nodes described the faces.

However, the SSM has the following shortcomings:

a) The SSM consists of nodes, faces, points, lines, surfaces, and entities, and as a result, these relationships become very complicated, occupy considerable storage space and consume excessive computing time.
b) The elements in the SSM have to be converted into nodes and faces for storage and presentation; as a result, the SSM is time consuming.

The SCSG-OSM proposed in this paper improves the SSM by avoiding its shortcomings. The details are below.

a) The OSM defines only four basic elements: point, line, face, and body. Moreover, the lines, faces, and bodies are represented using only point elements. As a result, the OSM largely reduces the procedures of identifying the nodes and surfaces. The OSM model occupies minimal storage space and is simple.
b) The OSM presents an object using a point set instead of nodes and/or surface elements. As a result, it largely reduces the time consumption during identification and conversion of the relationships in node-to-point and face-to-surface.
c) The definitions given in the SCSG-OSM specify the shape of an object, providing basic support for the topological relationships, which has been described in the "Section III.C".

IV. EXPERIMENTS

A. DATA SOURCES

This paper selects two datasets: Data set 1 (*hereafter called Dataset-1 in this paper*) is located in Denver, Colorado, USA. Data set 2 (*hereafter called Dataset-2 in this paper*) is located in Zurich, Switzerland, which was provided by the *International Society for Photogrammetry and Remote Sensing (ISPRS)*. The format in Dataset-1 is TXT, which records 3D coordinates of the buildings. Dataset-1 contains 100 buildings and a total of 4,452 points. Dataset-1 can be imported by using AutoCAD and can create lines and polygons in DXF format. Most buildings in Dataset-1 are located in the centre of the city, with high density, complex structures and rich textures. The detailed descriptions can be referenced in Zhou *et al.* [9]. Dataset-2 has 395 buildings and 20,821 points. The detailed descriptions can be referenced in the International Society for Photogrammetry and Remote Sensing (ISPRS) *https://www.isprs.org/data/hoengg/default.aspx*.

B. MODELLING BUILDINGS USING SCSG-OSM

The SCSG-OSM proposed above is carried out using virtual reality modelling language (VRML) developed by Silicon Graphics International (SGI). VRML 2.0 is an object-oriented 3D modelling language that can be used to build real-world scenes with platform independence. The specification of VRML 2.0 was adopted in August 1996 and open enough that anyone can experiment with problems in multi-user space. The details for our experiments are described below.

1) MODELLING A SINGLE BUILDING USING SCSG-OSM

To help understand the proposed SCSG-OSM, a building without texture (also called *"white mode"*) is taken as an example to explain the procedures. The steps are as follows:

- *Step-1*: A single building, denoted by *B001* (see Fig. 6 (a)), is selected as an example. In Fig. 6 (a) and Fig. 6 (b), B001 is composed of 8 bodies, *B001-1* through *B001-8*. B001 consists of walls, a roof and a bottom, in which B001-1 has 8 walls, 12 tops and 1 bottom; *B001-2*, which has a flat roof, has 5 walls, 1 top face and 1 bottom, where the bottom is shared with the bottom of B001-1F_{21}. The building roof has six components, B001-3, *B001-4*, *B001-5*, *B001-6*, *B001-7*, and *B001-8*. B001-3 is composed of F_{28} through F_{31}; *B001-4* through *B001-8* are composed of 3 walls and 3 top faces. *B001-8* consists of 3 walls and 1 top face.
- *Step-2*: In accordance with the definitions given in "Principle of the SCSG-OSM", building B001 can be defined using bodies, *i.e.*,

$$B001 = \{F_i^{bf}\} = \bigcup_{bf=1}^{k_1} F_i^{bf} = \bigcup_{bf=1}^{k_1} \bigcup_{fp=1}^{k_2} P_n^{bf,fp} \quad (45)$$

where $k_1 = 61$, $k_2 = 79$, *i.e.*,

$$B001 = \{F_1, \ldots, F_{61}\} = \{P_1, \ldots, P_{79}\} \quad (46)$$

In Fig. 6 (c), building B001 can be defined using lines, *i.e.*,

$B001 = \{L_i\} = \bigcup_{i=1}^{lpn} L_i = \bigcup_{i=1}^{k} \{P_n^{lp}\} = \bigcup_{i=1}^{lpn} \bigcup_{lp=1}^{k} P_n^{lp}$ where where $lpn = 132$, $k = 79$, *i.e.*,

$$B001 = \{L_1, \ldots, L_{132}\} = \{P_1, \ldots, P_{79}\} \quad (47)$$

This means that body B001 is the union of face F_1 thru F_{62} and is the union of points P_1 thru P_{79}. The points, lines, faces and bodies are stored in a relational database.

- *Step 3*: The 3D topological relationship given in OSM for B001 is as follows: B001-2 and B001-3 are disjoint. Refer to the representation of disjoint (R031) in "The 3D topological relationship in the SCSG-OSM" because of

$$\{\{F_{22}\}\ldots\{F_{27}\}\} = \partial B001-2, \{\{F_{28}\}\ldots\{F_{31}\}\} = \partial B001-3 \quad (48)$$

$$\left(\bigcup_{g=22}^{27} F_g\right) \cap \left(\bigcup_{h=28}^{31} F_h\right) = \emptyset \quad (49)$$

Then, B001-2 and B001-3 are disjoint. For B001-1 and B001-2, there are

$$\{\{F_1\}\ldots\{F_4\}\} = \partial \text{B001-2}, \{\{F_1\}\ldots\{F_4\}\} = B001-1^{\circ} \quad (50)$$

$$\bigcup_{g=1}^{4} F_g = \bigcup_{h=1}^{4} F_h, g = h \quad (51)$$

i.e., B001-1 and B001-2 overlap.

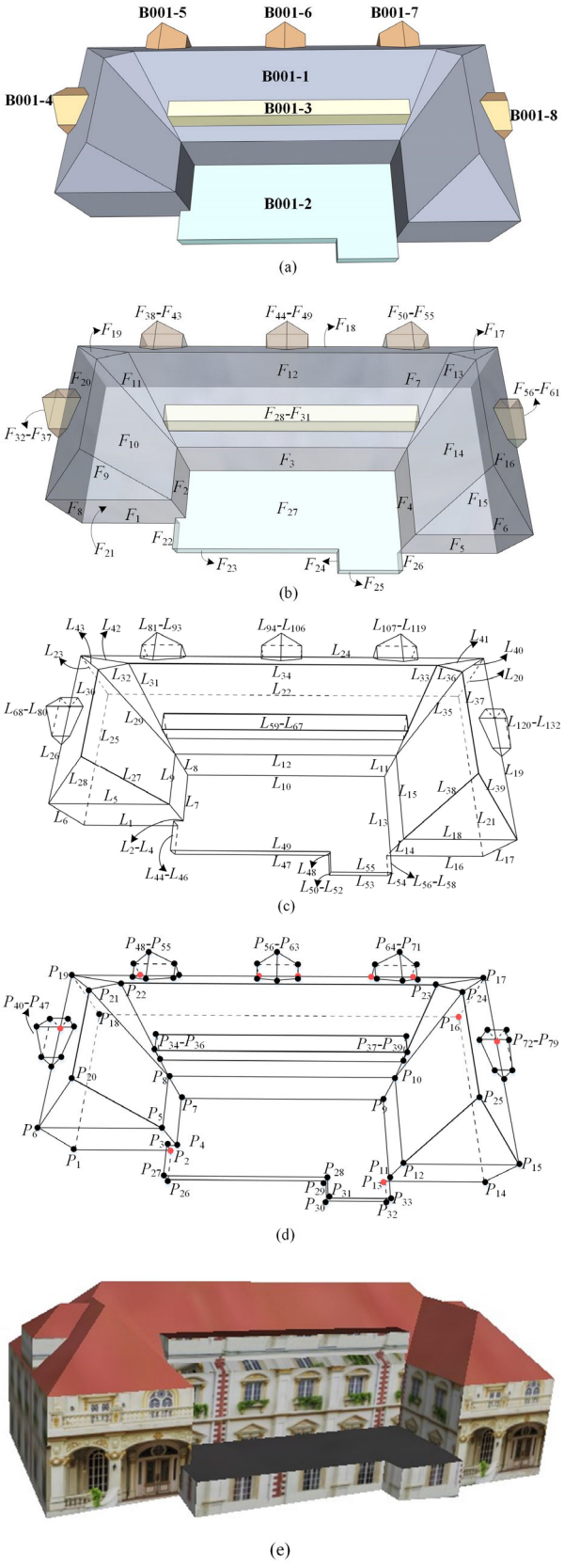

FIGURE 6. (a) Composition of building B001, (b) face representation of B001, (c) line representation of B001, (d) point representation of B001, and (e) B001 with real textures.

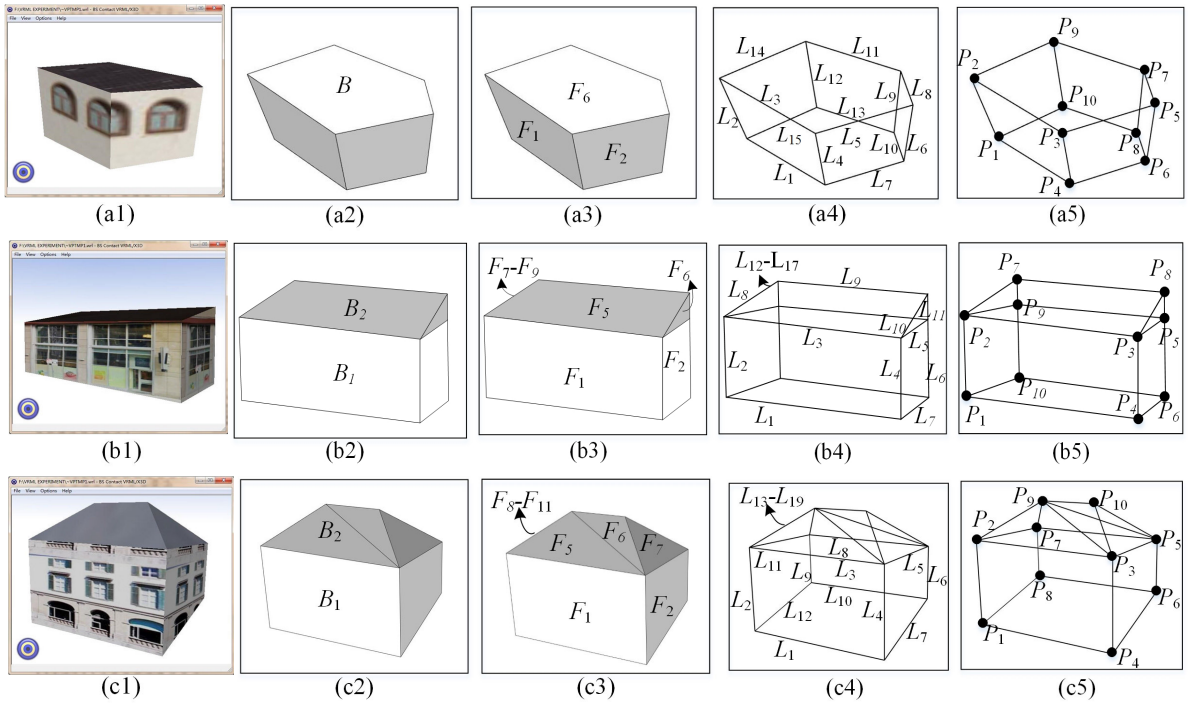

FIGURE 7. Different types of buildings and their representations using SCSG-OSM.

- *Step 4:* As described for data organization in "The Organization of Data Sets in the SCSG-OSM", the composite object (*CO*) can be represented by a group of point sets. Thus, texture images can be mapped onto building B001 using *ImageTexture* as an index, in which the coordinates of the texture image are from the point coordinates of the faces of B001, and the data, including faces and texture image, are read using *coordIndex*(coordinate index), *texcoordIndex* (texture coordinate index) and *normalIndex*(normal index). Finally, a single building is photorealistically created with real textures (see Fig. 6(e)).

2) MODELLING MULTIPLE BUILDINGS USING SCSG-OSM

a: MODELLING THREE TYPES OF BUILDINGS USING SCSG-OSM

The details of modelling a single building using the SCSG-OSM are given above. For modelling multiple buildings using the SCSG-OSM, similar procedures can be repeated. To further explain the procedures, three types of buildings, flat-roof, single-roof and multi-roof buildings, are taken as examples.

Fig. 7(a1) through Fig. 7(a5) represent the flat roof of a building, which consists of 10 points, 15 lines and 7 faces and is expressed by

$$B=\{B_1\}=\{F_1,\ldots,F_7\}=\{L_1,\ldots,L_{15}\}=\{P_1,\ldots,P_{10}\} \tag{52}$$

Fig. 7(b1) through Fig. 7(b5) represent the single roof of a building with 2 bodies, which consists of 10 points, 17 lines and 9 faces and can be expressed by

$$B=\{B_1,B_2\}=\{F_1,\ldots,F_9\}=\{L_1,\ldots,L_{17}\}=\{P_1,\ldots,P_{10}\} \tag{53}$$

Fig. 7(c1) through Fig. 7(c5) represent multiple roofs with 2 bodies, which consist of 10 points, 19 lines and 11 faces and can be expressed by

$$B=\{B_1,B_2\}=\{F_1,\ldots,F_{11}\}=\{L_1,\ldots,L_{19}\}=\{P_1,\ldots,P_{10}\} \tag{54}$$

b: MODELLING MULTIPLE BUILDINGS USING SCSG-OSM FOR DATASET-1

Dataset-1, located in the city of Denver, Colorado, USA, contains 100 buildings and 4,452 points. Most buildings are located in the centre of the city and have rich textures. The modelling steps are as follows:

- *Step-1:* We first define simple/complex objects as bodies in VRML. There are 100 bodies of building model for Dataset-1, which consist of 4,452 points, 2,624 lines and 2,454 faces in total. The faces include 100 top faces, 100 bottom faces and 2,254 wall faces, which can be represented by point sets. The building model can be defined as bodies:

$$\begin{aligned}&BuildingModel_{-1}=\{b_1,b_2,\ldots,b_{100}\}\\&=\{F_1,F_2,\ldots,F_{100}\}=\{\{f_1,f_2,\ldots,f_n\},\ldots,\{\ldots\},\{f_i,\ldots,f_{2454}\}\}\\&=\{L_1,L_2,\ldots,L_{100}\}=\{\{l_1,l_2,\ldots,l_n\},\ldots\{\ldots\},\{l_i,\ldots,l_{2624}\}\}\\&=\{P_1,P_2,\ldots,P_{100}\}=\{\{p_1,p_2,\ldots,p_n\},\ldots,\{\ldots\},\{p_i,\ldots,p_{4452}\}\}\end{aligned} \tag{55}$$

All these points, lines, faces and bodies are stored in a relational database as records. Each record has its unique ID, and they are associated by their IDs to describe their relationships.

- *Step 2:* The indexes, including *coord*, *IndexedFaceSet*, *facecoordIndex*, *ImageTexture*, *texcoordIndex* and *normalIndex*, are defined. The *coord* represents the point index of the point sets. The *IndexedFaceSet* represents the index of face sets that compose the bodies, and each face set contains many faces. The index of a face is named *facecoordIndex*, and each face is composed of the coordinates. *ImageTexture* presents the texture image index. The *texcoordIndex* represents the texture coordinate index. The texture coordinates are the same as the point coordinates of a face. The *normalIndex* represents the normal vector index. These indexes are used to record the IDs and coordinates of points, lines, faces, bodies and textures.
- *Step-3:* The points, lines, faces, bodies and textures are read through the coordinates of the indexes. Ninety-one images taken by the camera or screenshot from Google Earth are employed as the texture images. The texture images are attached to the faces of the building using the *texcoordIndex*.
- *Step 4:* The 3D building model for Dataset-1 is created. The final result is depicted in Fig. 8. The curved structure of the 3D model can be established when the curved surface contains enough points (see Fig. 8(b)).

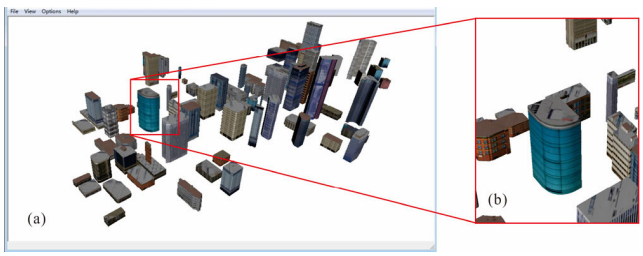

FIGURE 8. Building models using SCSG-OSM for Dataset-1 that depict the city of Denver, Colorado, USA.

C. MODELLING MULTIPLE BUILDINGS USING SCSG-OSM FOR DATASET-2

Dataset-2, located in the city of Zurich, Switzerland, has 395 buildings, which contains 20821 points. The buildings are located in the centre of the city, with complex structures and rich textures, especially rich roof structures. The same experiment is carried out as in Dataset-1. The building model for Dataset-2 is constructed as follows:

- *Step-1:* We define buildings as bodies first. There are 395 bodies for Dataset-2, which consist of 20,821 points, 13,506 lines and 17,269 faces. The faces include 395 top faces, 6,115 bottom faces and 10,759 wall faces, which can be represented by point sets. The building model can be defined as bodies:

$$\begin{aligned} BuildingModel_{-2} &= \{b_1, b_2, \ldots, b_{395}\} \\ &= \{F_1, F_2, \ldots, F_{395}\} = \{\{f_1, f_2, \ldots, f_n\}, \ldots, \{\ldots\}, \{f_i, \ldots, f_{17269}\}\} \\ &= \{L_1, L_2, \ldots, L_{395}\} = \{\{l_1, l_2, \ldots, l_n\}, \ldots \{\ldots\}, \{l_i, \ldots, l_{13506}\}\} \\ &= \{P_1, P_2, \ldots, P_{395}\} = \{\{p_1, p_2, \ldots, p_m\}, \ldots, \{\ldots\}, \{p_i, \ldots, p_{20821}\}\} \end{aligned} \tag{56}$$

All these points, lines, faces and bodies are stored in a relational database.

- *Step-2:* Repeat the same *Step 2* as in Dataset-1.
- *Step 3:* Eighty images taken by the camera and screenshot from Google Earth are employed as the texture image. The texture images are attached to the faces of the building with the same operation as *Step 2* for Dataset-1.
- *Step-4:* Finally, the 3D building model for Dataset-2 is created, and the final result is depicted in Fig. 9.

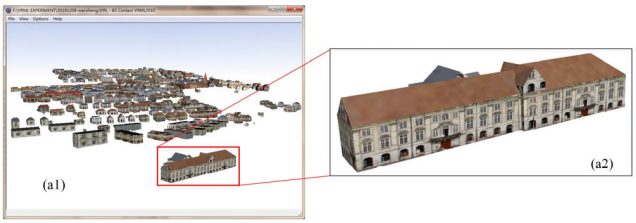

FIGURE 9. Building models using SCSG-OSM for Dataset-2 that depict the city of Zurich, Switzerland.

D. COMPARISON AND ANALYSIS

To evaluate the advantages and disadvantages of the SCSG-OSM proposed in this paper, six existing methods—the CSG-BR model, TIN model, POLYGON model, Patch model, SSM and CityGML model—are compared and analysed below.

1) CSG-BR MODEL

The modelling tool AutoCAD 2015 is applied to create all of the 3D building models for Dataset-1. AutoCAD 2015 was developed by Autodesk in 2015 and is able to draw 2D and 3D graphics. The geometric representations for 3D buildings in AutoCAD 2015 use the CSG-BR model. The details of the process are shown as follows.

For the Dataset-1 experiment, the points are input to AutoCAD 2015 to form the footprints of buildings, and then the footprints of the buildings are stretched to obtain the 3D building model using a stretching tool. The result is shown in Fig. 10(a). As observed from Fig. 10(a), all of the 3D building models through AutoCAD 2015 are without textures since AutoCAD 2015 does not support texture mapping.

2) TIN MODEL

The modelling tool ArcScene is applied to create all of the 3D building models for Dataset-1. ArcScene, developed by ESRI, is able to create realistic scenes and 3D models.

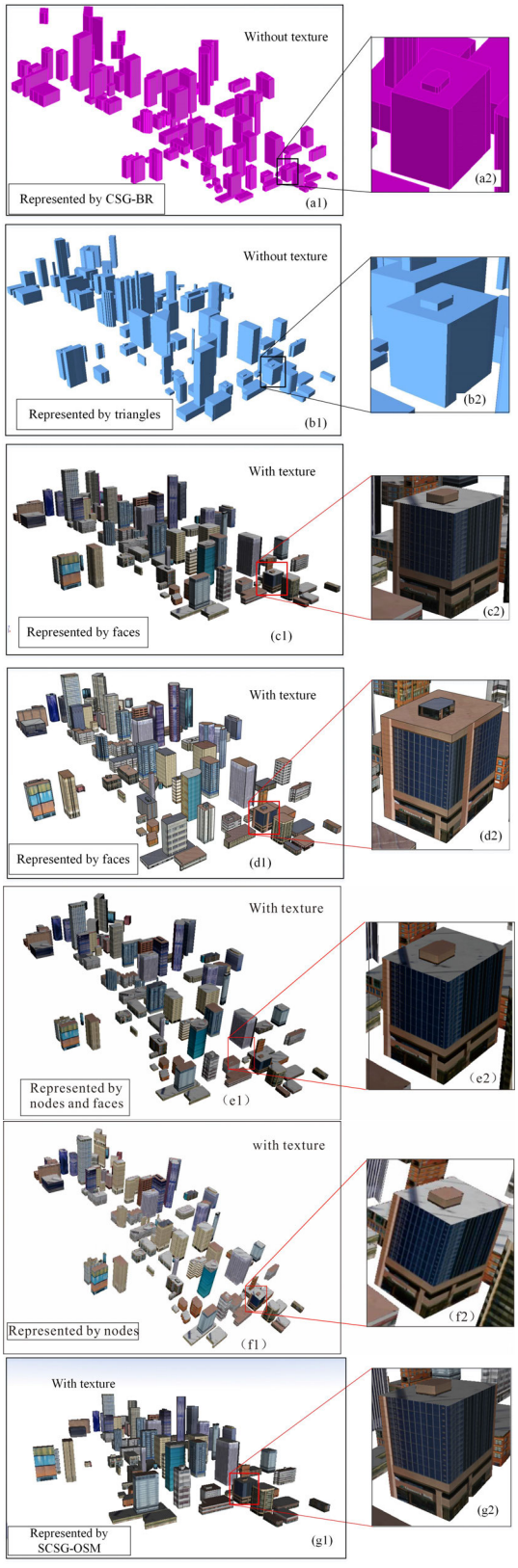

FIGURE 10. Modelling the buildings for Dataset-1 using seven methods: (a) CSG-BR model; (b) TIN model; (c) POLYGON model; (d) Patch model; (e) SSM; (f) CityGML model; (g) the proposed method.

The geometric representations for 3D buildings in ArcScene use the TIN model. The details of the process are shown as follows.

For the Dataset-1 experiment, the footprints of the buildings are input to ArcScene, and the heights are assigned to each footprint; then, the footprints of the buildings are stretched in accordance with the elevation. Finally, 3D building models are created, and the result is shown in Fig. 10(b). As observed in Fig. 10(b), all of the 3D building models through ArcScene are created without textures, since ArcScene does not support texture mapping.

3) POLYGON MODEL

The modelling tools in 3ds Max 2014 are applied to create all of the 3D building models for Dataset-1. The 3ds Max 2014 program is a professional modelling software developed by Autodesk in 2014 and is capable of creating realistic models and realizing image texture mapping. The geometric representations for 3D buildings in 3ds Max 2014 use the POLYGON model. The details of the process are shown as follows.

For the Dataset-1 experiment, the footprints of all buildings are constructed first using 3ds Max 2014, and then the stretching tool is employed to stretch the footprints in accordance with the height of the building. The roof model and details are constructed and modified accordingly to construct all of the 3D building models for Dataset-1. Finally, the material editor in 3ds Max 2014 is employed to map the texture images, and all the 3D buildings with real textures are obtained and are shown in Fig. 10(c).

4) PATCH MODEL

SketchUp 2015 is a 3D design software developed by Atlast-Software in 2015. SketchUp 2015 has a convenient *push-pull* function that makes it easy to generate 3D geometry with a single graphic. The geometric representation for 3D buildings in SketchUp 2015 uses the Patch model. The details of the process are shown as follows.

For the experiment for Dataset-1, the footprints of the buildings are constructed first in accordance with the point data in SketchUp 2015, and then the stretching tool is employed to stretch the footprints to the height of the building. Finally, 3D building models for Dataset-1 are constructed, and the material tool is employed to attach a texture image to each building wall. The results for all 3D buildings with real textures for Dataset-1 are created and depicted in Fig. 10(d).

5) SSM

The basic steps using the SSM to create the 3D buildings for Dataset-1 using VRML are as follows:

- First, the data of Dataset-1 are converted into nodes and faces and store them in a relational database as records.

- Second, the indexes of nodes, faces and image textures are established.
- Third, the 3D model of a building without wall textures is established by using nodes and faces.
- Finally, the texture images are attached onto the faces of the building using the texture index. The results for all 3D buildings with real textures for Dataset-1 are created and depicted in Fig. 10(e).
- CityGML model

CityGML provides modelling of all relevant parts of the virtual city according to their semantics, geometry, topology and appearance. An FME is a spatial data conversion processing system developed by Safe Software, Canada, which supports the reading and writing of CityGML appearances. The steps to generate the CityGML model using an FME are as follows:

- First, the.dwg file of Dataset-1 is read, and the number of times that each wall texture is pasted in the u/v (texture coordinate) direction is calculated.
- Second, the wall is stretched according to the building height.
- Finally, texture images of the wall and texture map are added according to the calculated number of times. The results for all 3D buildings with real textures for Dataset-1 are created and depicted in Fig. 10(f).

The SCSG-OSM proposed in this paper is applied to create all 3D buildings for Dataset-1 by VRML. The experimental steps have been described in ''Section IV.B.2''. The result is depicted in Fig. 10(g).

Repeating the same operations as for Dataset-2, the 3D building models employing the seven modelling methods are created, and their results are shown in Fig. 11(a), Fig. 11(b), Fig. 11(c), Fig. 11(d), Fig. 11(e), Fig. 11(f) and Fig. 11(g).

With the experimental results shown in Fig. 10 and Fig. 11, a few conclusions can be drawn as follows.

a) As observed from Fig. 10(a), Fig. 10(b), Fig. 11(a) and Fig. 11(b), the buildings are represented by bodies and lines in the CSG-BR model, while the buildings are represented by triangles in the TIN model. In addition, the models created using the CSG-BR model and TIN model in AutoCAD 2015 and ArcScene cannot show the reality of the building textures since the two software systems have no texture mapping functions.

b) As observed from Fig. 10(c), Fig. 11(c), Fig. 10(d), Fig. 11(d), Fig. 10(e), Fig. 11(e), Fig. 10(f) and Fig. 11(f), all of the buildings are textured, which means that all of the buildings are truly able to show the reality of buildings when using the POLYGON model, Patch model, SSM and CityGML model.

To further compare their characteristics, the model representations, storage space and the average time consumption when loading models are measured and analysed. The comparison analysis is conducted below:

a) *Comparison of representation elements:* The elements used for modelling the buildings for Dataset-1 and Dataset-2 for seven methods are analysed. The results are shown in Table 2 and Table 3.

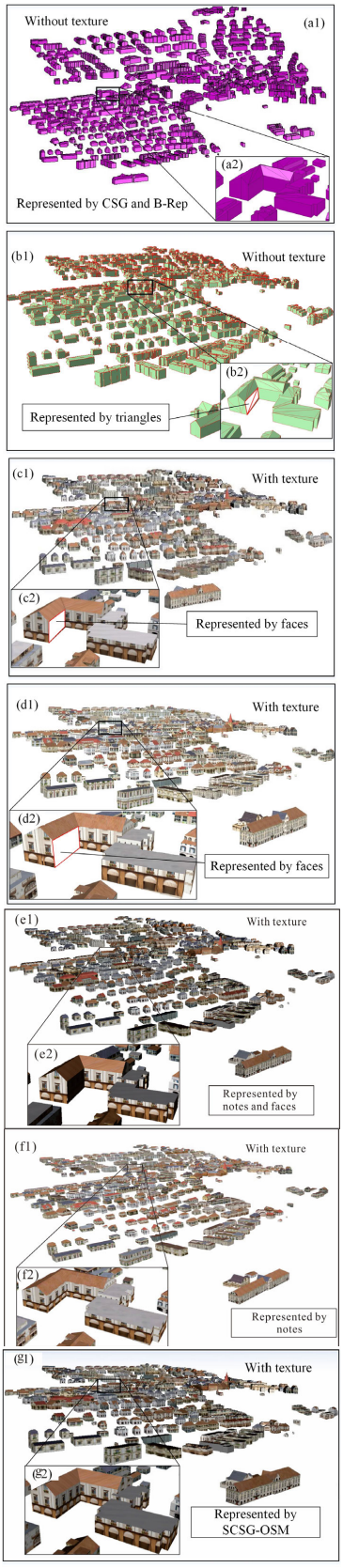

FIGURE 11. Modelling the buildings for Dataset-2 using seven methods: (a) CSG-BR model; (b) TIN model; (c) POLYGON model; (d) Patch model; (e) SSM; (f) CityGML model; (g) the proposed method.

TABLE 2. Comparison analysis with different models for Dataset-1.

Modelling methods	Representation elements	Storage space	Average time consumption	Texture or not
SCSG-OSM	Points	12.20 MB	2.61 seconds	With texture
SSM	Nodes and faces	13.40 MB	8.53 seconds	
CityGML model	Nodes	9.90 MB	15.13 seconds	
POLYGON model	Faces	12.35 MB	3.71 seconds	
Patch model	Faces	14.50 MB	4.43 seconds	
TIN model	Triangles	1.32 MB	2.56 seconds	Without texture
CSG-BR model	Bodies and lines	1.59 MB	4.67 seconds	

TABLE 3. Comparison analysis with different models for Dataset-2.

Modelling methods	Representation elements	Storage space	Average time consumption	Texture or not
SCSG-OSM	Points	8.93 MB	2.49 seconds	With texture
SSM	Nodes and faces	12.10 MB	6.13 seconds	
POLYGON model	Faces	10.40 MB	3.84 seconds	
CityGML model	Nodes	17.70 MB	28.56 seconds	
Patch model	Faces	9.73 MB	3.57 seconds	
TIN model	Triangles	13.70 MB	2.69 seconds	Without texture
CSG-BR model	Bodies and lines	9.07 MB	6.33 seconds	

b) *Comparisons of storage space:* The storage space occupied using the seven methods for Dataset-1 and Dataset-2 are compared and analysed, and the results are shown in Table 2 and Table 3, respectively.

c) *Comparisons of average time consumption:* To analyse the characteristics of the seven methods, the average time consumption when loading 3D building data for Dataset-1 and Dataset-2 are compared and analysed. The results are shown in Table 2 and Table 3.

As observed from Table 2 and Table 3, the following can be concluded:

a) The SCSG-OSM employs the element of point sets for representation of a 3D object, while other methods—the TIN model, CSG-BR model, SSM, CityGML model, POLYGON model, and Patch model—employ elements of triangles, bodies and lines, faces, nodes and faces and faces.

b) For Dataset-1, as observed in Table 2, the storage space required for our method is 12.2 MB, while the storage space required by the other methods—the TIN model, CSG-BR model, SSM, CityGML model, POLYGON model, and Patch model—are 1.32 MB, 1.59 MB, 13.40 MB, 9.90 MB, 12.35 MB and 14.50 MB, respectively. In addition, the average time consumed during model loading using our method is 2.61 seconds, with which the buildings are visualized using real textures; the average times consumed during the loading model with real textures when using the SSM, CityGML model, Patch model and POLYGON model are 8.53 seconds, 15.13 seconds, 4.43 seconds and 3.71 seconds. However, the average time consumed during model loading without textures when using the TIN model and CSG-BR model is 2.56 seconds and 4.67 seconds, respectively.

c) For Dataset-2, as observed in Table 3, the storage space required by our method is 8.93 MB, while storage space required by the other methods—the TIN model, CSG-BR model, SSM, CityGML model, POLYGON model, and Patch model—are 13.70 MB, 9.07 MB, 12.10 MB, 17.70 MB, 10.40 MB and 9.73 MB, respectively. In addition, the average time consumed during model loading using our method is 2.49 seconds, with which the buildings are visualized using real textures; the average times consumed during the loading model with real textures when using the SSM, CityGML model, Patch model and POLYGON model are 6.13 seconds, 28.56 seconds, 3.57 seconds and 3.84 seconds, respectively. However, the average time consumed during model loading without textures when using the TIN model and CSG-BR model modelling is 2.69 seconds and 6.33 seconds, respectively.

The experimental results above demonstrate that the data structure in the SCSG-OSM proposed in this paper is the simplest and the easiest to model, and the SCSG-OSM consumes the least time of all the methods.

V. CONCLUSIONS

In the past 10 years, many scholars have proposed a number of methods for modelling urban 3D buildings. However, previous 3D modelling methods have encountered bottlenecks due to their shortcomings in the efficiency of representing 3D photorealistic city models. The SSM is effective for the spatial visualization and query of 3D buildings, which converts the points, lines, surfaces and bodies into nodes and faces but suffers from excessive time consumption. Therefore, this paper proposes an SCSG-OSM method based on the SSM. The SCSG-OSM is constructed through points, lines, faces and bodies. The SCSG-OSM considers an object consisting of four element types: point, line, face, and body. Then, the four types of elements are strictly defined by nine basic definitions, in which lines, faces, and bodies are essentially described by point sets rather than by nodes and faces employed in the SSM. Finally, two data sets that depict the locations of Denver, Colorado, USA, and Zurich, Switzerland, provided by the *International Society for Photogrammetry and Remote Sensing (ISPRS)*, are used to validate our model.

A comparison analysis is also conducted with the CSG-BR model, TIN model, POLYGON model, Patch model, SSM and CityGML model. The comparisons illustrate the following:

(1) The elements representing a 3D object using SCSG-OSM are point sets, while the elements of the TIN model, CSG-BR model, SSM, CityGML model, POLYGON

model, and Patch model are triangles, bodies and lines, nodes and faces, nodes, faces and faces, respectively.

(2) For Dataset-2, the storage space required using SCSG-OSM is 8.93 MB, while 13.7 MB, 9.07 MB, 12.10 MB, 17.70 MB, 10.40 MB and 9.73 MB, respectively, was required when using the TIN model, CSG-BR model, SSM, CityGML model, POLYGON model, and Patch model. This implies that the data structure in the SCSG-OSM is the simplest of all the models.

(3) For Dataset-2, the SCSG-OSM is able to reduce the computational time by 7.43%, 60.66%, 59.38%, 91.28%, 35.16% and 30.25% compared to the TIN model, CSG-BR model, SSM, CityGML model, POLYGON model and Patch model, respectively. This implies that SCSG-OSM consumes the least computational time.

In summary, the experimental results demonstrate that the SCSG-OSM proposed in this paper is the simplest model, occupies the least amount of storage space and consumes less computational time than the TIN model, CSG-BR model, SSM, POLYGON model and Patch model.

In the future, we plan to develop a storage method of texture data in the database to improve the speed of texture image mapping and 3D reality visualization. In addition, this paper focuses only on the modelling of 3D buildings. We will try to solve the modelling of 3D buildings with multisource data.

REFERENCES

[1] C. Liang, "Real-time generation and rendering of urban building scenes based on scanned surfaces," M.S. thesis, Dept. Comput. Sci. Eng., South China Univ. Technol., Guangdong, China, 2010.

[2] Y. Liang, "Research on 3D model reconstruction of building from close range image sequence," Ph.D. dissertation, Dept. Cartography Geographic Inf., Nanjing Normal Univ., Jiangsu, China, 2013.

[3] S. Zlatanova, "3D GIS for urban development," Ph.D. dissertation, Dept. Civil Eng., Graz Univ. Tech., Graz, Austria, Mar. 2000.

[4] S. Zlatanova, A. A. Rahman, and W. Shi, "Topological models and frameworks for 3D spatial objects," *Comput. Geosci.*, vol. 30, no. 4, pp. 419–428, May 2004.

[5] G. Vosselman and I. Suveg, "Automatic 3D building reconstruction," in *Proc. SPIE Int. Soc. Opt. Eng.*, 2002, vol. 4661, no. 4661, pp. 59–69.

[6] B. Mao and L. Harrie, "Methodology for the efficient progressive distribution and visualization of 3D building objects," *ISPRS Int. J. Geo-Inf.*, vol. 5, no. 10, p. 185, Oct. 2016.

[7] G. Zhou, Y. Huang, T. Yue, X. Li, W. Huang, C. He, and Z. Wu, "Hybrid modeling based on SCSG-BR and orthophoto," in *Proc. ISPRS Tech. Commission III Midterm Symp. 'Develop., Technol. Appl. Remote Sens.*, Beijing, China, 2018, pp. 2575–2579.

[8] G. Zhou, C. Song, J. Simmers, and P. Cheng, "Urban 3D GIS from LiDAR and digital aerial images," *Comput. Geosci.*, vol. 30, no. 4, pp. 345–353, May 2004.

[9] G. Zhou, W. Chen, J. A. Kelmelis, and D. Zhang, "A comprehensive study on urban true orthorectification," *IEEE Trans. Geosci. Remote Sens.*, vol. 43, no. 9, pp. 2138–2147, Sep. 2005.

[10] G. Zhou, Z. Tan, M. Cen, and C. Li, "Customizing visualization in three-dimensional urban GIS via Web-based interaction," *J. Urban Planning Develop.*, vol. 132, no. 2, pp. 97–103, Jun. 2006.

[11] G. Zhou and X. Zhou, "Seamless fusion of LiDAR and aerial imagery for building extraction," *IEEE Trans. Geosci. Remote Sens.*, vol. 52, no. 11, pp. 7393–7407, Nov. 2014.

[12] H. Ledoux and M. Meijers, "Topologically consistent 3D city models obtained by extrusion," *Int. J. Geographical Inf. Sci.*, vol. 25, no. 4, pp. 557–574, Apr. 2011.

[13] K. Sugihara, "Knowledge-based automatic generation of 3D building models from building footprint by straight skeleton computation," *Int. J. Knowl. Web Intell.*, vol. 3, no. 4, pp. 361–371, 2012.

[14] K. Sugihara and Z.-J. Shen, "Automatic generation of 3D building models by rectification of building polygons," *Adv. Sci. Lett.*, vol. 21, no. 12, pp. 3649–3654, Dec. 2015.

[15] B. Xiong, M. Jancosek, S. Oude Elberink, and G. Vosselman, "Flexible building primitives for 3D building modeling," *ISPRS J. Photogramm. Remote Sens.*, vol. 101, pp. 275–290, Mar. 2015.

[16] K. Ohori, H. Ledoux, F. Biljecki, and J. Stoter, "Modeling a 3D city model and its levels of detail as a true 4D model," *ISPRS Int. J. Geo-Inf.*, vol. 4, no. 3, pp. 1055–1075, Jul. 2015.

[17] X. Sun, Q. Li, and B. Yang, "Compositional structure recognition of 3D building models through volumetric analysis," *IEEE Access*, vol. 6, pp. 33953–33968, 2018.

[18] T. H. Kolbe, G. Gröger, and L. Plümer, Eds., "CityGML: Interoperable access to 3D city models," in *Geo-Information for Disaster Management*. Berlin, Germany: Springer-Verlag, 2005, pp. 883–899.

[19] M. Elmekawy, A. Östman, and K. Shahzad, "Towards interoperating CityGML and IFC building models: A unified model-based approach," in *Adv. 3D Geo-Information Sciences*, T. H. Kolbe, G. König, and C. Nagel, Eds. New York, NY, USA: Springer, 2011, pp. 73–93.

[20] G. Gröger and L. Plümer, "CityGML—Interoperable semantic 3D city models," *ISPRS J. Photogram.*, vol. 71, pp. 12–33, Jul. 2012.

[21] C. Dore and M. Murphy. (2012). Integration of HBIM and 3D GIS for Digital Heritage Modelling. Dublin Institute of Technology. [Online]. Available: https://arrow.tudublin.ie/cgi/viewcontent.cgi?article=1071&context=beschreccon

[22] M. Goetz, "Towards generating highly detailed 3D CityGML models from OpenStreetMap," *Int. J. Geographical Inf. Sci.*, vol. 27, no. 5, pp. 845–865, May 2013.

[23] J. Slade, C. B. Jones, and P. L. Rosin, "Automatic semantic and geometric enrichment of CityGML building models using HOG-based template matching," in *Advances in 3D Geoinformation*, A. R. Alias, Ed. New York, NY, USA: Springer, 2017, pp. 357–372.

[24] H. Fan, L. Meng, and M. Jahnke, "Generalization of 3D buildings modelled by CityGML," in *Proc. Agile Conf.*, Hannover, Germany, 2009, pp. 387–405.

[25] B. Mao, Y. Ban, and L. Harrie, "A multiple representation data structure for dynamic visualisation of generalised 3D city models," *ISPRS J. Photogramm. Remote Sens.*, vol. 66, no. 2, pp. 198–208, Mar. 2011.

[26] H. Fan and L. Meng, "A three-step approach of simplifying 3D buildings modeled by CityGML," *Int. J. Geographical Inf. Sci.*, vol. 26, no. 6, pp. 1091–1107, Jun. 2012.

[27] S. U. Baig and A. A. Rahman, "A three-step strategy for generalization of 3D building models based on CityGML specifications," *GeoJournal*, vol. 78, no. 6, pp. 1013–1020, Dec. 2013.

[28] F. Biljecki, H. Ledoux, J. Stoter, and J. Zhao, "Formalisation of the level of detail in 3D city modelling," *Comput., Environ. Urban Syst.*, vol. 48, pp. 1–15, Nov. 2014.

[29] F. Biljecki, H. Ledoux, J. Stoter, and G. Vosselman, "The variants of an LOD of a 3D building model and their influence on spatial analyses," *ISPRS J. Photogramm. Remote Sens.*, vol. 116, pp. 42–54, Jun. 2016.

[30] F. Biljecki, H. Ledoux, and J. Stoter, "An improved LOD specification for 3D building models," *Comput., Environ. Urban Syst.*, vol. 59, pp. 25–37, Sep. 2016.

[31] F. Biljecki, H. Ledoux, and J. Stoter, "Generating 3D city models without elevation data," *Comput., Environ. Urban Syst.*, vol. 64, pp. 1–18, Jul. 2017.

[32] Y. Deng, J. C. P. Cheng, and C. Anumba, "Mapping between BIM and 3D GIS in different levels of detail using schema mediation and instance comparison," *Autom. Construct.*, vol. 67, pp. 1–21, Jul. 2016.

[33] L. Li, F. Luo, H. Zhu, S. Ying, and Z. Zhao, "A two-level topological model for 3D features in CityGML," *Comput., Environ. Urban Syst.*, vol. 59, pp. 11–24, Sep. 2016.

[34] Y. Zheng, Q. Weng, and Y. Zheng, "A hybrid approach for three-dimensional building reconstruction in Indianapolis from LiDAR data," *Remote Sens.*, vol. 9, no. 4, p. 310, Mar. 2017.

[35] K. Chen, F. Xue, and W. Lu, "Development of 3D building models using multi-source data," in *Proc. Joint Conf. Comput. Construct. (JC3)*, Heraklion, Greece, 2017, pp. 611–618.

[36] A. A. Diakité, G. Damiand, and D. V. Maercke, "Topological reconstruction of complex 3D buildings and automatic extraction of levels of detail," in *Proc. Eurograph. Workshop Urban Data Modeling Vis.*, Goslar, Germany, 2014, pp. 25–30.
[37] M. Löwner, J. Benner, G. Gröger, and K. Häfele, "New concepts for structuring 3D city models—An extended level of detail concept for CityGML buildings," in *Proc. Int. Conf. Comput. Sci. Appl.*, Ho Chi Minh City, Vietnam, 2013, pp. 466–480.
[38] K. Chen, W. Lu, F. Xue, P. Tang, and L. H. Li, "Automatic building information model reconstruction in high-density urban areas: Augmenting multi-source data with architectural knowledge," *Autom. Construction*, vol. 93, pp. 22–34, Sep. 2018.
[39] F. Xue, K. Chen, D. Liu, Y. Niu, and W. S. Lu, "An optimization-based semantic building model generation method with a pilot case of a demolished construction," in *Proc. 21st Int. Symp. Advancement Construct. Manage. Real Estate*, Hong Kong, 2018, pp. 231–241.
[40] Q. Wang, "Research on the application of new tilt aerial photography technology in city modeling," M.S. thesis, Dept. Surveying Geographic Inf., Lanzhou Jiaotong Univ., Gansu, China, 2013.
[41] H. Li, "Research and analysis of 3D modeling and visualization technology of digital city," M.S. thesis, Dept. Civil Hydraulic Eng., Hefei Univ. Technology, Anhui, China, 2013.
[42] D. Zhang, "The application of close-range photogrammetry and 3D rendering technology in building fine modeling," M.S. thesis, Dept. Inf. Sci. Eng., Shandong Agricult. Univ., Shandong, China, 2015.
[43] C. Ma, "3D geometric modeling of urban buildings based on a single high-resolution remote sensing image," M.S. thesis, Dept. Geosci. Environ. Eng., Southwest Jiaotong Univ., Sichuan, China, 2012.
[44] R. Zhang, H. Ai, L. Zhang, and Q. Wang, "A novel method for semi-automatic complex building reconstruction under additional conditional constraints," *Bull. Surv. Mapping*, vol. 11, pp. 64–68, Nov. 2015.
[45] S. Zlatanova and M. Gruber, "3D urban GIS on the Web: Data structuring and visualization," in *Proc. ISPRS, Commission*, Stuttart, Germany, 1998, pp. 691–699.
[46] M. J. Egenhofer, "Deriving the composition of binary topological relations," *J. Vis. Lang. Comput.*, vol. 5, no. 2, pp. 133–149, Jun. 1994.

GUOQING ZHOU (Senior Member, IEEE) received the Ph.D. degree from Wuhan University, Wuhan, China, in 1994. He was a Visiting Scholar with the Department of Computer Science and Technology, Tsinghua University, Beijing, China, and a Postdoctoral Researcher with the Institute of Information Science, Beijing Jiaotong University, Beijing. He continued his research as an Alexander von Humboldt Fellow with the Technical University of Berlin, Berlin, Germany, from 1996 to 1998, and was a Postdoctoral Researcher with The Ohio State University, Columbus, OH, USA, from 1998 to 2000. He was an Assistant Professor, an Associate Professor, and a Full Professor with Old Dominion University, Norfolk, VA, USA, in 2000, 2005, and 2010, respectively. He has authored or coauthored six books, seven book chapters, and more than 400 peer-refereed publications.

TAO YUE is currently pursuing the Ph.D. degree with the Guilin University of Technology, Guilin, China. He has published 50 articles and three software copyrights. His research interests include the generation of true orthophoto and 3-D modeling of urban buildings.

YU HUANG received the M.S. degree in surveying and mapping from the Guilin University of Technology, Guilin, China, in 2019. She has been working with Nanning Exploration and Survey Geoinformation Institute, Guangxi, China, since 2019.

BO SONG is currently pursuing the M.S. degree. He will start a new academic career as the Ph.D. Student with the Guilin University of Technology, Guilin, China, in August 2020.

KUNSHAN CHEN (Fellow, IEEE) received the Ph.D. degree in electrical engineering from The University of Texas at Arlington, in 1990. From 1992 to 2014, he was a Professor with National Central University, Taiwan. From 2014 to 2019, he was with the Institute of Remote Sensing and Digital Earth, Chinese Academy of Sciences, China. Since 2019, he has been with the Guilin University of Technology as a National Distinguished Professor. He has authored or coauthored over 160 refereed journal articles and contributed ten book chapters. He has been a member of the Editorial Board of IEEE Access, since 2020.

HONGCHANG HE received the Ph.D. degree from the University of Fribourg, Switzerland, in 2000. His research interests include remote sensing and GIS applications to ocean, agriculture, and environment.

JINSHENG NI received the Ph.D. degree from Beijing University, in 2009. His research interests include intelligent processing and information extraction of remote sensing satellite data, big data storage, and cloud service architecture.

LIQIANG ZHANG (Member, IEEE) received the Ph.D. degree in geoinformatics from the Institute of Remote Sensing Applications, Chinese Academy of Sciences, Beijing, China, in 2004. He is currently a Professor with the Faculty of Geographical Science, Beijing Normal University, Beijing. His research interests include remote sensing image processing, 3-D urban reconstruction, and spatial object recognition.

QIUYU PAN, photograph and biography not available at the time of publication.